Journal of Research in Science Engineering and Technology
Volume 8, Issue 4, November 2020, pp. 50-59

Journal of Research in Science Engineering and Technology

www.researchub.org

Refractive Index Sensor for Detection of N_2, He and CO_2 Gases based on Square Resonance Nanocavity in 2D Photonic Crystal

Parisa Sami[1], Mojtaba Hosseinzadeh Sani[2] *, Hadi Behzadnia[3], Chao Shen[4]

[1, 2, 4] Faculty of Electronic and Information Engineering, Xi'an Jiaotong University, China
[3] State key Laboratory of Multiphase Flow in Power Engineering, Xi'an Jiaotong University, China

Abstract

In this work, the design and simulation of high-sensitivity gas optical sensor (GOS), based on photonic crystals with refractive index different of linear materials is presented. The lattice index is cubic and the dielectric rods are made of silicon and are designed in a square shape. In the proposed optical sensor, three resonance nanocavities are used, the central nanocavity is made of silicon with a refractive index of $n_{Si} = 2.6$, and the sub-nanocavities located in the path of the input waveguide and the output waveguide This optical sensor is able to detection of N_2, He and CO_2 gases from the air. Numerical simulation results are obtained using two-dimensional FDTD method. The use of three resonance nanocavities and the distances between the dielectric rods increased the sensitivity and quality factor of the structure. The proposed optical sensor has a sensitivity of S = 400 nm/RIU and a quality factor of Q.f = 1080.615, and the power transmission is about T_E = 100%. The figure of merit is equal to FOM = 258.333 ± 8.333 RIU^{-1}. It is designed to integrate the structure with small dimensions as much as possible. The overall dimensions of the structure are 72.6 μm^2, which can be easily used in optically integrated circuits.

Keywords

Gas Optical Sensor (GOS), Photonic Crystals, Square Nanocavity, High-Sensitivity.

1. Introduction

The last two decades have seen a significant increase in research related to photon crystal-based optical sensors (Joannopoulos et al., 2008; Malmir & Fasihi, 2007; Nair & Vijaya, 2010; Zhao et al., 2011). Photon crystal gas sensors with micro-scale and nano-scale dimensions are significantly sensitive

* Corresponding author: Faculty of Electronic and Information Engineering, Xi'an Jiaotong University, China
E-mail Address: mojtabasani69@gmail.com.

Received 30 August 2020 / Accepted 28 October
DOI: https://doi.org/10.24200/jrset.vol8iss04pp50-59

to refractive index changes and are one of the basic elements in all-optical systems. These types of sensors can be designed in two method: 1- In the first case, dielectric rods are placed in the air substrate and the sensor works by spreading gas and changing the air refractive index, which is used in this article. 2- The second method is to place air holes in the slab substrate, which is easier in terms of fabrication (Sünner et al., 2008; Feng et al., 2012; Bougriou et al., 2013; Kumar et al., 2015). Photonic crystals, which are alternating structures of electromagnetic materials, have an optical band gap, small size, low fabricated cost during mass production, the ability to integrate with other optically integrated devices and circuits, and a high operating frequency range with high pedestrian capability. They have very compact sensors. All-optical structures based on photonic crystals, in addition to gas sensors, have a variety of structures used in optical circuits, such as optical biosensors (Sani & Khosroabadi, 2020), accelerometers sensors (Sani et al., 2020a), ultrafast nonlinear half-adder (Sani et al., 2020b; Saghaei et al., 2017), Analog to Digital (Sani et al., 2020c; 2020d), and Filters (Sani et al., 2020e).

So far, a lot of research has been done in this field. By carefully selecting the structural parameters of a photonic crystal, such as the lattice index value, the dimensions of the air cavities and the type of substrate, the characteristics of the optical band gap can be controlled. Xiao & Mortensen (2007) developed a new sensor-liquid with a sensitivity of 498 nm / RIU based on the scattering of photonic crystal algebras. Morshed et al. (2015) Introduced a gas detection sensor with defective core PCO based on silica doped GeO2. It provides 27.58% for the methane (CH4) and hydrogen fluoride (HF) gas adsorption lines with λ = 1.33 μm. In the same year, Morshed & Singh (2015) introduced a modified hexagonal PCF based on pure silica for gas metering applications. Islam et al. (2017) proposed a single-mode helical PCF-based gas sensor that increases the sensitivity response to gas detection. The sensor response at light wavelength λ = 1.33 μm was 57.61% (Islam et al., 2017). In 2020, another fiber optic gas sensor was introduced by Bikash Kumar Paul et al. that the sensor shows the sensitivity responses of 64.69% and confinement loss of 4.38×10^{-06} dB/cm at the transmission wavelength λ =1.55 μm. As it was observed, many structures have been presented with different methods with different results. In this paper, the structure is proposed to detect several types of gas based on three square nanocavities (Paul et al., 2020).

2. Band Structure

The base of the proposed structure is designed as a cubic lattice index with square dielectric rods. The photon crystal under study consists of dielectric rods in the air Substrate. The photon crystal lattice constant is a = 550 nm. In Figure 1, section (a) shows the refractive index difference between the dielectric rod and the substrate air the dielectric rods are selected as square and with $X_{(Scale)} = Z_{(Scale)} =$ 137.5 nm dimensions, and section (b) shows the Brilluoin zone and Kpath for a square dielectric rod. As can be seen in this figure, the refractive index increases from n=1 (air) to n = 4.2. However, it should be noted that, the refractive index is calculated as epsilon ($\varepsilon=n^2$) (See Figure 1).

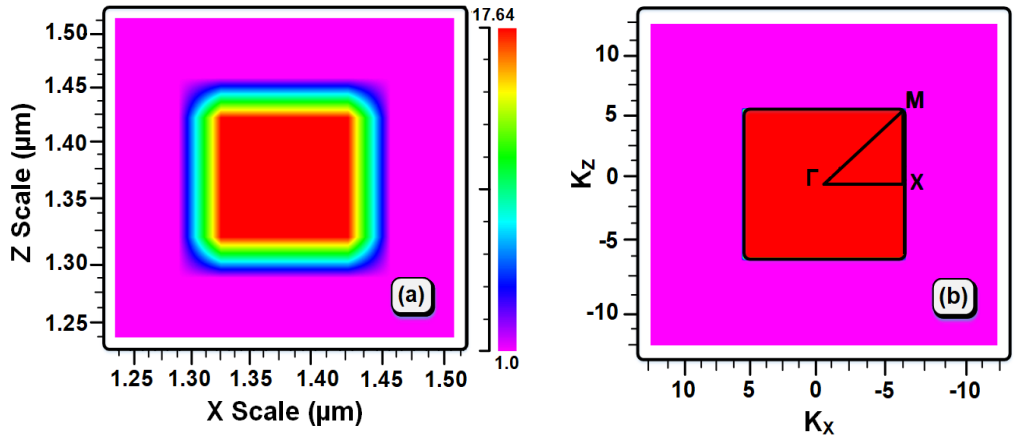

Fig. 1. Show band structure result, (a) two-dimensional dielectric constant profile at Y=0, (b) Brillouin zone and Kpath.

By choosing the right lattice index and dielectric sizes, it creates the right frequency range in the normal frequency range of laser sources and telecommunication. Examining the frequency contour curves of the photon crystal optical band diagram modes, and by identifying the region in which the contour size decreases with increasing frequency, it can be concluded that this photon crystal structure operates only in the magnetic polarization mode. Figure 2 (a) shows the photonic bandgap range. This frequency range is in the range of a/λ = 0.296 ~ 0.461 and the wavelength range of the structure is between λ = 1.193 μm ~ 1.839 μm. Therefore, if the input optical signal is applied to the structure in this frequency range, the light will be reopened, and if the optical signal is applied to the structure outside this frequency range, it will be propagated in the structure. Figure 2 (b) clearly shows the effects of polarization mode of the input light signal. As shown in Figure 2, if an optical signal is applied to the structure in an electric polarization mode (TE), light is scattered in the structure. But if an optical signal is applied to the structure with a magnetic polarization mode (TM), the light will be reopened and will not penetrate into the structure. Therefore, it can be concluded that the proposed structure performs well in the state of magnetic polarization mode (TM).

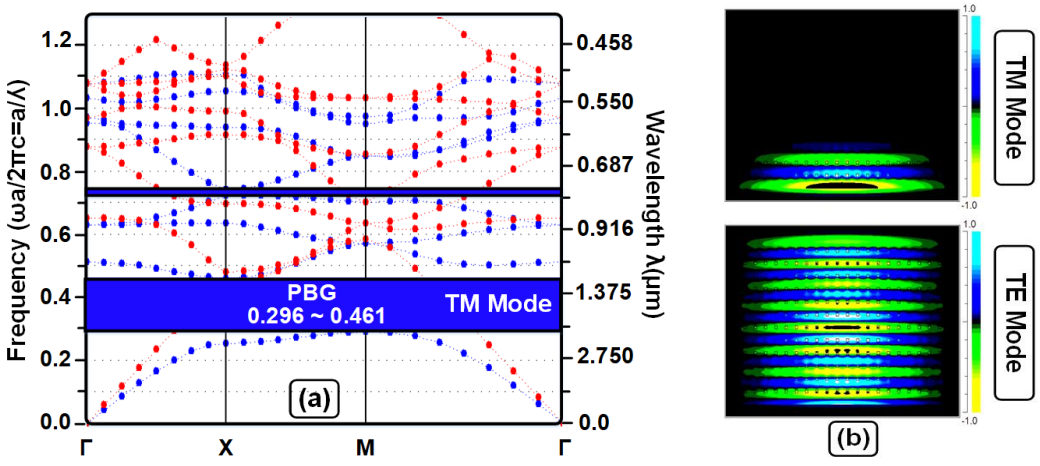

Fig. 2. (a) Photonic bandgap diagram, (b) Transmissions of TM mode and TE mode.

3. Gas Optical Sensor (GOS)

The proposed structure is designed and simulated based on 2D photon crystals for detection of Helium (He), Nitrogen (N_2) and Carbonic (CO_2) gases. Figure 3 shows the proposed structure of the gas optical sensor (GOS). The black dielectric rods are made of glioma and dimensions is equal to $X_{(Scale)} = Z_{(Scale)} = 137.5$ nm. The pink resonance nanocavity is located in the center of the structure, the size of this square nanocavity is equal to $X_{(Scale)} = Z_{(Scale)} = 687.5$ nm. The green resonance nanocavity is located in the around of center nanocavity, the size of this square nanocavity is equal to $X_{(Scale)} = Z_{(Scale)} = 550$ nm. This sensor has an input waveguide and an output waveguide and the detection is based on the refractive index of the gases. The operation of the structure is such that normally the dielectric rods are located in the air substrate and there is a laser source in the input waveguide which is always scattering the signal to the input of the structure, and the optical signal with a wavelength Special received from output waveguide. When the gas leaks into the structure, it will change the refractive index of the air, which by 3 nanocavities shifted wavelength. Another important parameter in the design of optical structures is the overall dimensions. In this design, an attempt has been made to select the minimum amount of dimensions that the overall dimensions of the structure are equal to 72.6μm^2. The designed structure has very suitable dimensions for integration and use in optically integrated circuits.

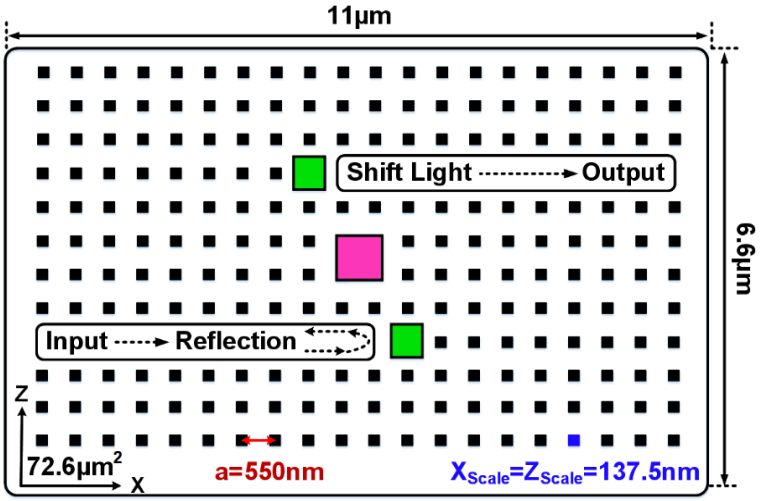

Fig. 3. Propose of Gas Optical Sensor (GOS).

At this stage we want to examine the structure in normal condition and when there is air in the structure, calculate the amount of resonant wavelength and other important parameters such as quality factor and minimum bandwidth. Figure 4 (a) shows the resonant wavelength obtained for the normal state. As can be seen, the transmissions power in this case is equal to $TE_{(Air)} = 98\%$ and the resonant wavelength is equal to $\lambda_{(Air)} = 1.296732$ μm^2. Figure 4 (b) shows the transmissions power in logarithm (dB scale) to calculate the exact minimum bandwidth. As shown in Figure 4, to calculate the FWHM parameter, we go -3dB below the signal peak and this parameter is equal to FWHM = 6.3nm. The value of quality factor for normal mode is calculated by equation (1).

$$Q.f = \frac{\lambda_0}{FWHM} \quad (1)$$

Another important parameter of sensors is the quality factor, which is directly related to sensitivity, and the higher the value, the better. where λ_0 is the resonance wavelength, which is the same as $\lambda_{(Air)}$ for this case. Using this formula, the quality factor is equal to Q.f = 205.83.

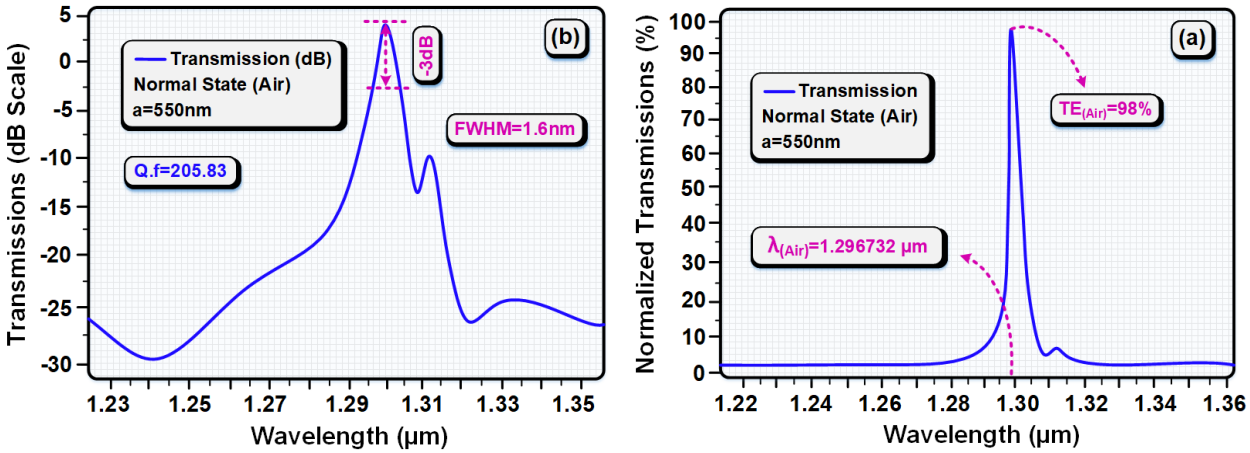

Fig. 4. (a) Normalized Transmissions, (b) Transmissions (dB Scale).

Up to this point, the main parameters of the sensor were examined to show that the design was performed quite properly. The proposed structure was tested for the normal state or Air substrate and the resonant frequency was obtained with good values, and no gas detection has been done yet.

4. Simulation Results

In this section, we analysis the structure designed to test He, N_2 and CO_2 gases. We will enter the gases into the structure in order and analyze the specifications and results. As mentioned earlier, the detection in the proposed sensor is based on the refractive index of the gases. Table 1 shows the very exact values of air and gas refractive index.

Table 1. Refractive index of air and gases studied.

Samples	Refractive Index
Air	1.000265
Helium (He)	1.000032
Nitrogen (N_2)	1.000270
Carbonic (CO_2)	1.000407

As can be seen in Table 1, the lowest refractive index is related to helium (He) gas and the highest refractive index is related to carbonic dioxide (CO_2) gas. In this section, we base the air and compare the gases with the air. Figure 5 (a) examines the detection in the normal state with the nitrogen (N_2) gas leaking. As can be seen, the sensor receives an optical signal with a resonant wavelength of $\lambda_{(Air)}$ = 1.296732 μm from the output in the normal state. When the nitrogen (N_2) gas leaks, the resonant wavelength shifts and receives a value of $\lambda_{(Air)}$ = 1.296734 μm from the output. $\Delta\lambda$ which is the distance between these two resonant frequencies, is equal to $\Delta\lambda$ = 0.002 nm. The average bandwidth and quality factor are FWHM = 1.5 nm and Q.f = 864.48, respectively. The important parameters of sensitivity and shape of competence for this case are calculated as S = 400 nm/RIU and FOM = 258.333 ± 8.333 RIU^{-1}, respectively. According to the results obtained for this case, it can be concluded that with the leakage of nitrogen gas, the quality factor and the resonance wavelength in the structure have increased and

the average bandwidth has decreased. Figure 5 (b) shows the calculations and analyzes for when helium (He) gas leaks into the structure. Due to the fact that the refractive index of helium gas is lower than air, the amount of resonance wavelength is less than the normal (air) state, which the resonance wavelength for this state is equal to $\lambda_{(He)}$ = 1.296720 μm. One of the parameters obtained with a good value in this detection is the amount of transmission power and when helium gas leaks, the structure can transmit $TE_{(He)}$ = 100% of the optical signal to the output. The distance between the two resonant wavelengths is also equal to 3, and it can be concluded that the higher distance between the resonant wavelengths received from the output of the structure, the lower the sensitivity and figure of merit values, which are equal to or S = 51.5 nm/RIU and FOM = 30.399 ± 1.788 RIU^{-1}, respectively. Figure 5 (c) shows the results for when carbon dioxide (CO_2) leaks into the structure. Because the average amount of bandwidth in this case has reached the lowest value, it has caused the quality factor to reach the maximum value in this case. The average bandwidth in this case is FWHM = 1.2 nm, which has resulted in a quality factor of Q.f= 1080.615. The sensitivity in this case is equal to S = 39.7 nm/RIU.

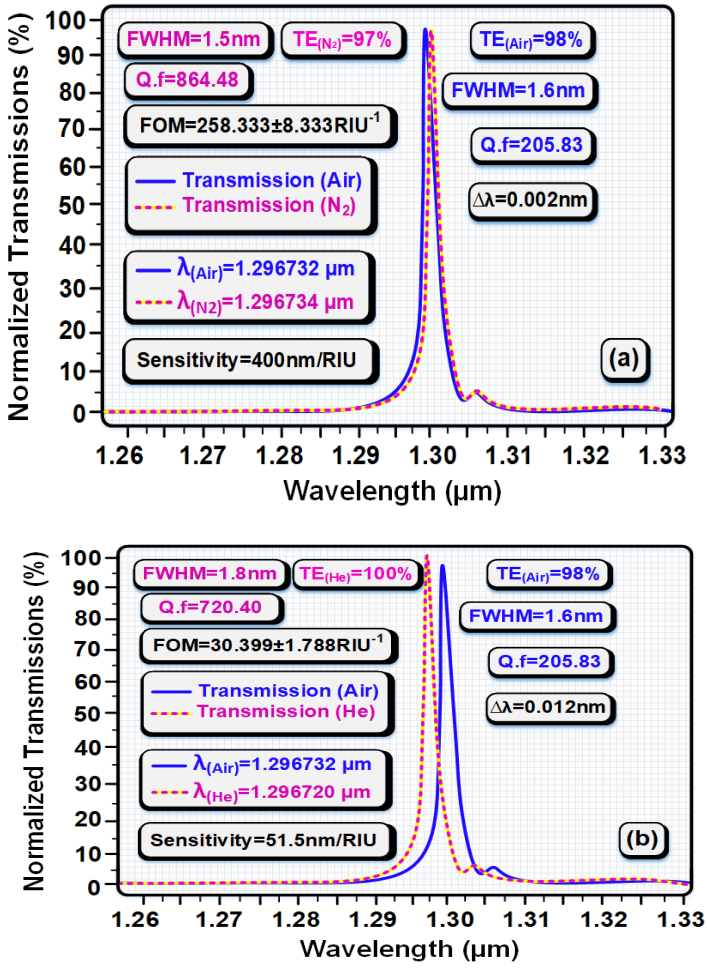

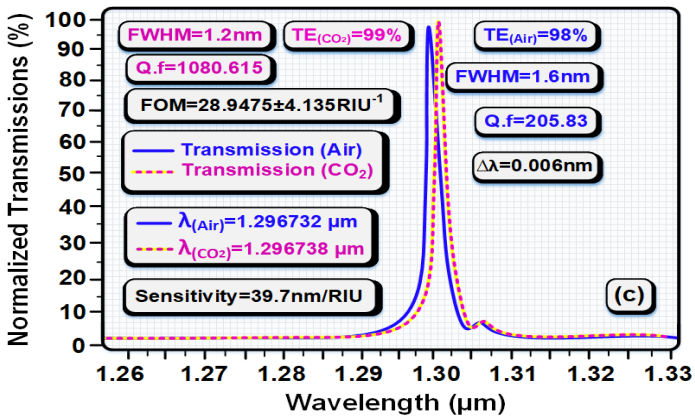

Fig. 5. Normalized transmission power for gas leaks, (a) nitrogen (N_2), (b) Helium (He), (c) carbon dioxide (CO_2).

According to the results obtained in different cases, we can conclude that the structure designed for when nitrogen gas leaks, we achieve the best amount of sensitivity and figure of merit. and when carbon dioxide leaks into the structure, we get the lowest average bandwidth and the highest quality factor from the structure output. Finally, when helium gas leaks into the structure, the proposed structure can transfer all the power of the incoming optical signal to the output of the structure, reducing the power loss to zero.

In this section, to prove that we have selected the best sizes of center nanocavities (pink color) and around of nanocavities (green color), we have reviewed and analyzed the proposed structure in different dimensions of nanocavities. As can be seen in Figure 6 (a), the amount of resonant wavelength increases with increasing comparison of the central (pink) nanocavity, and on the other hand, by increasing this scale to $X_{(Scale)} = Z_{(Scale)} = 710$ nm, the quality factor decreases and with further increase of the nanocavity scale, the quality factor increases. According to Figure 6, it can be concluded that the best quality factor has been calculated on the scale of $X_{(Scale)} = Z_{(Scale)} = 687.5$ nm. In Figure 6 (b), the parameters of the average value of bandwidth and transmission power are calculated according to different scales of the central nanocavity. The transfer power parameter decreases with increasing nanoscale resonance scale and the parameter of the average value of bandwidth is inversely related to the quality factor and reaches its maximum value in comparison with $X_{(Scale)} = Z_{(Scale)} = 710$ nm and decreases again. According to the obtained results, it can be concluded that the best scale for the central nanocavity is $X_{(Scale)} = Z_{(Scale)} = 687$, which will reach the highest quality factor and transfer power.

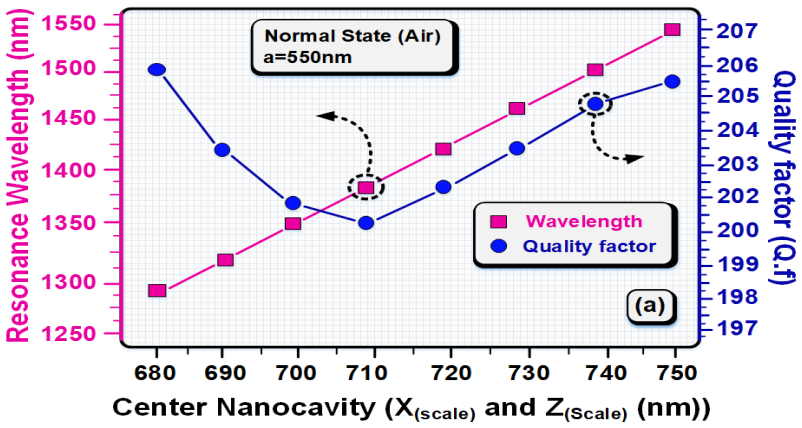

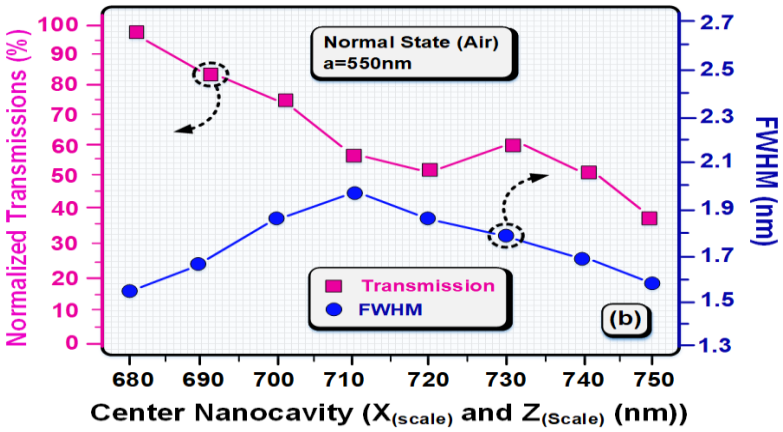

Fig. 6. (a) Calculation of quality factor and resonant wavelength parameters in terms of central nanocavity scale, (b) Calculation of transmissions power and FWHM parameters in terms of central nanocavity scale.

In this section we want to examine the sensitivity ratio on the Δλ parameter. At each step, we calculated the optical signals with specific resonance wavelengths with different refractive index, and then we examined a sensitivity for both optical signals and recorded the results. As can be seen in Figure 7, the highest sensitivity is related to the state in which helium gas has leaked into the structure, and in other states and other refractive indexes, the sensitivity changes in the range of 30 nm/RIU to 60 nm/RIU.

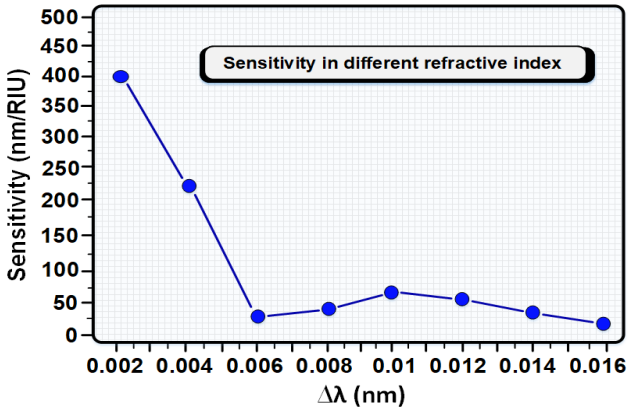

Fig. 7. Calculate the sensitivity at different refractive indices in Δλ (nm).

In the final part, we want to examine the proposed structure in both active and inactive modes. In Figure 8 (a), the structure is inactive. In this case, we applied an optical signal with an amplitude of λ = 1.382512 μm to the structure, in which case it transmits only 6% of the power to the output of the structure and creates TE = 94% of the power loss. In Figure 8 (b), the structure is active because we have applied an optical signal with an amplification wavelength of λ = 1.296720 μm to the structure, which has transmitted TE = 100% of the power to the output of the structure, and the power loss in this state has reached zero.

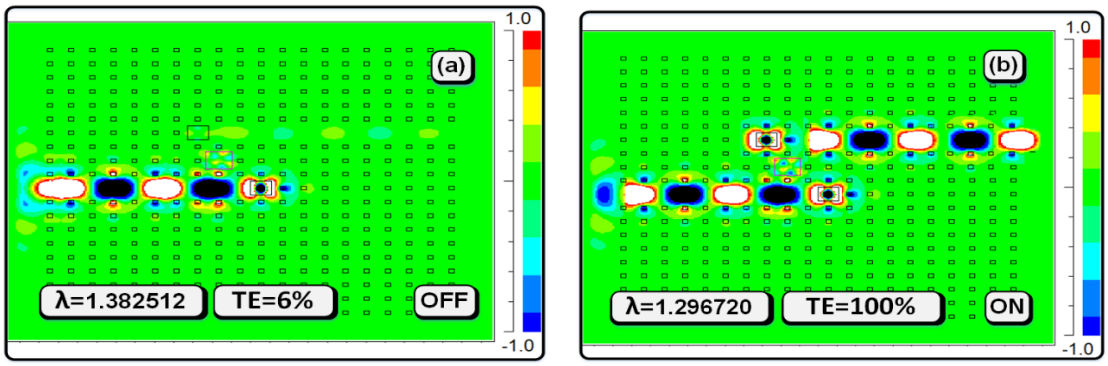

Fig. 8. (a). Sensor function in passive mode with wavelength λ = 1.382512. (b). Sensor function in active mode with wavelength λ = 1.296720.

5. Conclusion

In this article, we have designed a sensor with high quality factor and sensitivity, that can detect 3 types of gas from the air. At each stage, with gas leakage inside the structure and changing the refractive index of the substrate structure, the resonance wavelength received from the output changed, which is the main reason for the performance of the proposed structure. Power losses in helium gas detection have reached zero and the transmission power is 100%. The sensitivity is calculated in the range of S = 30 nm/RIU to S = 400 nm/RIU and the figure of merit is equal to FOM = 258.333 ± 8.333 RIU^{-1} at best. The quality factor, calculated in the best case equal to Q.f = 1080.615. The proposed structure can easily detect different gases with refractive index in the range of RI = 0.00032 to RI = 0.00407 with high sensitivity. The overall dimensions of the structure are 72.6 μm^2, which can be easily used in integrated optical circuits.

References

Bougriou, F., Bouchemat, T., Bouchemat, M., & Paraire, N. (2013). Optofluidic sensor using two-dimensional photonic crystal waveguides. *The European Physical Journal Applied Physics, 62*(1), 11201. https://doi.org/10.1051/epjap/2013110442

Feng, C., Feng, G., Zhou, G., Chen, N., & Zhou, S. (2012). Design of an ultracompact optical gas sensor based on a photonic crystal nanobeam cavity. *Laser Physics Letters, 9*(12), 875-878. https://doi.org/10.7452/lapl.201210075

Islam, I., Paul, B. K., Ahmed, K., Hasan, R., Chowdhury, S., Islam, S., . . . Asaduzzaman, S. (2017). Highly birefringent single mode spiral shape photonic crystal fiber based sensor for gas sensing applications. *Sensing and bio-sensing research, 14*(1), 30-38. https://doi.org/10.1016/j.sbsr.2017.04.001

Joannopoulos, J. D., Johnson, S. G., Winn, J. N., & Meade, R. D. (2008). *Molding the flow of light*. Princeton University Press.

Kumar, A., Saini, T. S., & Sinha, R. K. (2015). Design and analysis of photonic crystal biperiodic waveguide structure based optofluidic-gas sensor. *Optik, 126*(24), 5172-5175. https://doi.org/10.1016/j.ijleo.2015.09.157

Malmir, N., & Fasihi, K. (2017). A highly-sensitive label-free biosensor based on two dimensional photonic crystals with negative refraction. *Journal of Modern Optics, 64*(20), 2195-2200. https://doi.org/10.1080/09500340.2017.1346828

Morshed, M. G., & Singh, A. E. (2015). Recent trends in the serologic diagnosis of syphilis. *Clinical and vaccine immunology, 22*(2), 137-147.

Morshed, M., Hassan, M. I., Roy, T. K., Uddin, M. S., & Razzak, S. A. (2015). Microstructure core photonic crystal fiber for gas sensing applications. Applied Optics, 54(29), 8637-8643. https://doi.org/10.1364/AO.54.008637

Nair, R. V., & Vijaya, R. (2010). Photonic crystal sensors: An overview. *Progress in Quantum Electronics, 34*(3), 89-134. https://doi.org/10.1016/j.pquantelec.2010.01.001

Paul, B. K., Ahmed, K., Dhasarathan, V., Al-Zahrani, F. A., Aktar, M. N., Uddin, M. S., & Aly, A. H. (2020). Investigation of gas sensor based on differential optical absorption spectroscopy using photonic crystal fiber. *Alexandria Engineering Journal*. https://doi.org/10.1016/j.aej.2020.09.030

Saghaei, H., Zahedi, A., Karimzadeh, R., & Parandin, F. (2017). Line defects on As2Se3-Chalcogenide photonic crystals for the design of all-optical power splitters and digital logic gates. *Superlattices and Microstructures, 110*(1), 133-138. https://doi.org/10.1016/j.spmi.2017.08.052

Sani, M. H., & Khosroabadi, S. (2020). A novel design and analysis of high-sensitivity biosensor based on nano-cavity for detection of blood component, diabetes, cancer and glucose concentration. *IEEE Sensors Journal*. 10.1109/JSEN.2020.2964114

Sani, M. H., Ghanbari, A., & Saghaei, H. (2020e). An ultra-narrowband all-optical filter based on the resonant cavities in rod-based photonic crystal microstructure. *Optical and Quantum Electronics, 52*(1), 295.

Sani, M. H., Khosroabadi, S., & Nasserian, M. (2020d). High performance of an all-optical two-bit analog-to-digital converter based on Kerr effect nonlinear nanocavities. *Applied Optics, 59*(4), 1049-1057. https://doi.org/10.1364/AO.379575

Sani, M. H., Khosroabadi, S., & Shokouhmand, A. (2020c). A novel design for 2-bit optical analog to digital (A/D) converter based on nonlinear ring resonators in the photonic crystal structure. *Optics Communications, 458*(1), 124760. https://doi.org/10.1016/j.optcom.2019.124760

Sani, M. H., Saghaei, H., Mehranpour, M. A., & Tabrizi, A. A. (2020a). A Novel All-Optical Sensor Design Based on a Tunable Resonant Nanocavity in Photonic Crystal Microstructure Applicable in MEMS Accelerometers. *Photonic Sensors*, 1-15. https://doi.org/10.1007/s13320-020-0607-0

Sani, M. H., Tabrizi, A. A., Saghaei, H., & Karimzadeh, R. (2020b). An ultrafast all-optical half adder using nonlinear ring resonators in photonic crystal microstructure. *Optical and Quantum Electronics, 52*(2), 107. https://doi.org/10.1007/s11082-020-2233-x

Sünner, T., Stichel, T., Kwon, S.-H., Schlereth, T., Höfling, S., Kamp, M., & Forchel, A. (2008). Photonic crystal cavity based gas sensor. *Applied Physics Letters, 92*(26), 261112. https://doi.org/10.1063/1.2955523

Xiao, S., & Mortensen, N. A. (2007). Proposal of highly sensitive optofluidic sensors based on dispersive photonic crystal waveguides. *Journal of Optics A: Pure and Applied Optics, 9*(9), 463-467. https://doi.org/10.1088/1464-4258/9/9/S30

Zhao, Y., Zhang, Y.-N., & Wang, Q. (2011). Research advances of photonic crystal gas and liquid sensors. *Sensors and Actuators B: Chemical, 160*(1), 1288-1297. https://doi.org/10.1016/j.snb.2011.09.064